JCB Report

Regulation of SNAREs by tomosyn and ROCK: implication in extension and retraction of neurites

Toshiaki Sakisaka, Takeshi Baba, Shintaro Tanaka, Genkichi Izumi, Masato Yasumi, and Yoshimi Takai

Department of Molecular Biology and Biochemistry, Osaka University Graduate School of Medicine/Faculty of Medicine, Suita, Osaka 565-0871, Japan

Extension of neurites requires the SNARE-dependent fusion of plasmalemmal precursor vesicles with the plasma membrane of growth cones. Here, we show that tomosyn localizes at the palm of growth cones and inhibits the fusion of the vesicles there, thus promoting transport of the vesicles to the plasma membrane of the leading edges of growth cones. Tomosyn localizes because ROCK activated by Rho small G protein phosphorylates syntaxin-1, which increases the affinity of syntaxin-1 for tomosyn and forms a stable complex with tomosyn, resulting in inhibition of the formation of the SNARE complex. In retraction of neurites, tomosyn localizes all over the edges of the neurites and inhibits fusion of the vesicles with the plasma membrane. Thus, tomosyn demarcates the plasma membrane by binding to syntaxin-1 phosphorylated by ROCK, and thereby regulates extension and retraction of neurites.

Introduction

Formation and extension of axons and dendrites (so-called neurite outgrowth) is a crucial event in neuronal differentiation and maturation during development of the nervous system (Horton and Ehlers, 2003). Neurons first form several neurites, one of which becomes an axon and extends (Goslin and Banker, 1989). Extension of axons relies primarily on transport and addition of new components to the plasma membrane. Membrane expansion at the tips of extending axons is accomplished by the fusion of plasmalemmal precursor vesicles with the plasma membrane of growth cones (Futerman and Banker, 1996). SNAREs are essential molecules for membrane fusion in general, and the SNARE complex, consisting of t-SNAREs (syntaxin-1 and SNAP-25) and v-SNARE (VAMP-2), plays an important role in fusion of the vesicles with the plasma membrane of axons (Chen and Scheller, 2001). However, t-SNAREs broadly localize along the plasma membrane of axons, including growth cones and shafts, and the fusion of the vesicles might occur anywhere along the plasma membrane (Garcia et al., 1995). Therefore, there must be an exclusive machinery that targets the vesicles to the leading edges of growth cones.

We have previously identified a brain-specific Lgl family protein, named tomosyn, as a syntaxin-1–binding protein (Fujita et al., 1998). Tomosyn forms a complex with syntaxin-1 and SNAP-25 (Fujita et al., 1998). Here, we report that tomosyn serves as an exclusive machinery that targets the vesicles to the leading edges of growth cones.

Results and discussion

Tomosyn contains a large NH_2-terminal domain with WD40 repeats homologous to the Lgl family proteins and a COOH-terminal domain homologous to VAMP-2 (Fujita et al., 1998; Masuda et al., 1998; Fig. 1 A, a). To examine possible involvement of tomosyn in neurite outgrowth, we examined whether overexpression of tomosyn affects it in primary cultured rat hippocampal neurons and NG108 cells differentiated into neuron-like cells by dibutyryl cyclic AMP (db-cAMP; Nirenberg et al., 1983). Hippocampal neurons were transfected with HA-tagged full-length tomosyn (HA-tomosyn) or HA alone as a control. Hippocampal neurons formed neurites, but neurites from the neurons transfected with HA-tomosyn were fewer and shorter than those of the control cells (Fig. 1 A, b). Similar results were obtained for NG108 cells. The length and the number of neurites per cell was measured in each HA-positive NG108 cell. HA-tomosyn reduced the number of neurites longer than 50 μm and strongly increased the number of cells lacking neurites (Fig.

Address correspondence to Yoshimi Takai, Dept. of Molecular Biology and Biochemistry, Osaka University Graduate School of Medicine/Faculty of Medicine, Suita, Osaka 565-0871, Japan. Tel.: (81) 6-6879-3410. Fax: (81) 6-6879-3419. email: ytakai@molbio.med.osaka-u.ac.jp

Key words: tomosyn; ROCK; syntaxin; SNAREs; neurite outgrowth

Abbreviations used in this paper: db-cAMP, dibutyryl cyclic AMP; LPA, lysophosphatidic acid; MTs, microtubules; ROCK, Rho-associated serine/threonine kinase; siRNA, small interfering RNA.

The Journal of Cell Biology, Volume 166, Number 1, July 5, 2004 17–25
http://www.jcb.org/cgi/doi/10.1083/jcb.200405002

The Journal of Cell Biology

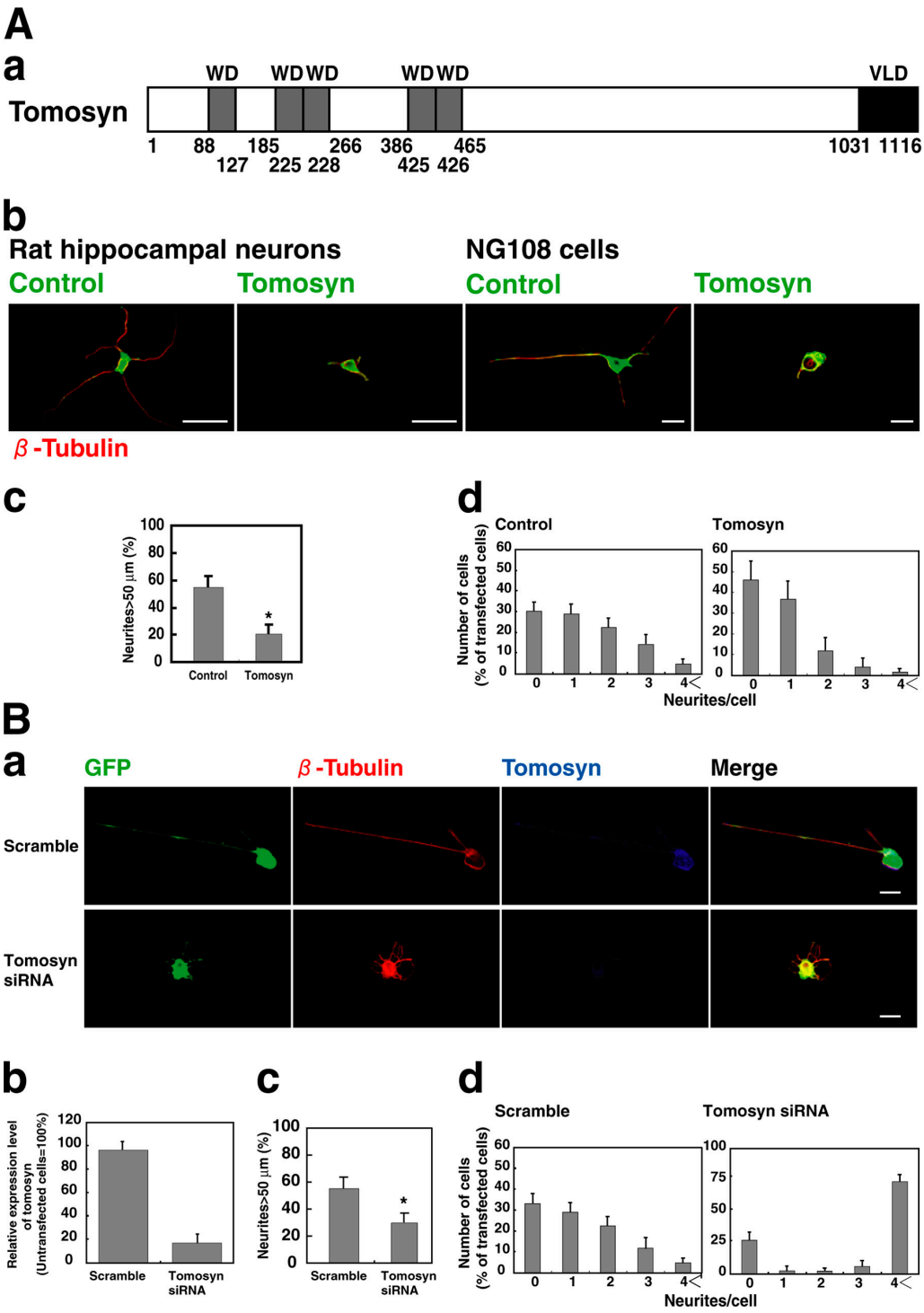

Figure 1. **Inhibition of neurite outgrowth by tomosyn.** (A) Effect of overexpression of tomosyn. (Aa) Schematic structure of tomosyn. Gray box (WD), WD40 repeats domain. Black box (VLD), VAMP-like domain. (Ab) Primary cultured rat hippocampal neurons were transfected with HA-tomosyn or a null HA plasmid (Control) and were cultured for 24 h. NG108 cells were transfected with HA-tomosyn or a null HA plasmid (Control), cultured in DME containing 1 mM db-cAMP for 48 h, and allowed to extend neurites. Overexpressing cells were identified by immunostaining of HA (green), and their MT structures were examined by immunostaining of β-tubulin (red). Bars, 20 μm. (Ac) Quantitative analysis of the neurite length of NG108 cells. Percentage of neurites longer than 50 μm. The mean value (± SEM) of percentage of neurites longer than 50 μm from three independent experiments is shown. *, $P < 0.01$ (*t* test). (Ad) Quantitative analysis of the number of neurites per cell of NG108 cells. The number of cells, expressed as the percentage of 100 transfected cells bearing 1, 2, 3, or >4 neurites is shown. The mean value (± SEM) of three independent experiments is shown. (B) Effect of tomosyn knock-down by the RNA interference method. (Ba) NG108 cells were transfected with the plasmid expressing both tomosyn siRNA and GFP or the plasmid expressing both scramble siRNA and GFP (Scramble), cultured in DME containing 1 mM db-cAMP for 48 h, and allowed to extend neurites. The cells expressing tomosyn or scramble siRNA were identified by the expression of GFP (green). Their MT structures were examined by immunostaining of β-tubulin (red) and the extent of expression of tomosyn (blue) was examined by immunostaining of tomosyn. Bars, 20 μm. (Bb) Quantification of the effect of tomosyn

1 A, c and d). Then, we knocked down endogenous tomosyn by the RNA interference method. Tomosyn knockdown cells had more sprouting neurites that were shorter than those of the control cells (Fig. 1 B, a–d). In addition, there was increased branching of neurites. These results indicate that tomosyn is involved in neurite outgrowth.

Then, we examined how this activity of tomosyn is regulated. Rho small G protein and its downstream target protein kinase, Rho-associated serine/threonine kinase (ROCK), regulate the actomyosin-based contractility and thereby induce collapse of growth cones and retraction of neurites (Bito et al., 2000; Da Silva et al., 2003). Because it is critical for these events to stop the addition of membrane to the leading edges of growth cones, we assumed that the Rho–ROCK system is related to the inhibitory effect of tomosyn on neurite outgrowth. Overexpression of myc-tagged ROCK-Δ3 (myc-ROCK-Δ3), a constitutively active mutant of ROCK, decreased the number of neurites and shortened them in hippocampal neurons and NG108 cells, whereas overexpression of myc-C3, a potent Rho-inhibiting enzyme, conversely increased the number of neurites and extended them moderately (Fig. 2, A–C). Cotransfection of myc-C3 with HA-tomosyn reduced neurite outgrowth. Overexpression of myc-ROCK KDIA, a RhoA binding-defective and kinase-dead mutant of ROCK that works as a dominant-negative form of ROCK, increased neurite outgrowth, and this effect was reduced by overexpression of tomosyn. Y27632, a specific ROCK inhibitor, showed a similar effect, and this effect was reduced by overexpression of tomosyn. In contrast, cotransfection of myc-ROCK-Δ3 with HA-tomosyn reduced neurite outgrowth potently. These results indicate that the activity of tomosyn is regulated by ROCK.

Next, we examined whether tomosyn inhibits neurite outgrowth by affecting vesicle transport to the plasma membrane. For this purpose, we examined the effect of tomosyn on VSV-G transport to the cell surface in NG108 cells. VSV-G is a membrane protein encoded by vesicular stomatitis virus, which is transported to the cell surface along the exocytotic pathway (Hirschberg et al., 1998). Export of VSV-G from the TGN was scored by immunofluorescence microscopy. In NG108 cells, exogenously expressed GFP-tagged VSV-G (GFP-VSV-G) accumulated in perinuclear regions, presumably the Golgi complex, by incubation at 20°C for 2 h, and was transported to the cell surface by incubation at 37°C for 1 h (Fig. 3 A). Overexpression of HA-tomosyn markedly inhibited this transport of GFP-VSV-G to the cell surface. Overexpressed tomosyn localized on the plasma membrane. Thus, tomosyn is likely to inhibit the fusion of the VSV-G–containing vesicles with the plasma membrane. This role of tomosyn was confirmed by the biochemical assay. NG108 cells were cotransfected with VSV-G and either HA-tomosyn or HA alone as a control. The kinetics of radiolabeled VSV-G transported to the cell surface was scored by cell surface biotinylation. When tomosyn was not exogenously expressed, VSV-G was detected at the cell surface within a 15-min chase period and increased steadily up to 1 h (Fig. 3 B). After a 1-h chase period, ~35% of total labeled VSV-G protein reached the cell surface. When HA-tomosyn was coexpressed with VSV-G, there was a noticeable decrease in the cell surface delivery at all time points. After a 1-h chase period, only ~10% of total labeled VSV-G reached the cell surface. Overexpression of myc-ROCK-Δ3 also inhibited the transport of GFP-VSV-G or VSV-G to the cell surface (Fig. 3, A and B). Because tomosyn forms the tomosyn complex, overexpression of tomosyn might inhibit the formation of the SNARE complex, which is essential for the fusion of the plasmalemmal precursor vesicles with the plasma membrane of growth cones. Therefore, we examined this possibility by measuring the amounts of HA-tomosyn and VAMP-2 that were coimmunoprecipitated with syntaxin-1 from the lysates of the cells overexpressing HA-tomosyn and the control cells. Both HA-tomosyn and VAMP-2 were coimmunoprecipitated with syntaxin-1 in both cells, but the amount of coimmunoprecipitated VAMP-2 in the cells overexpressing HA-tomosyn was far less than that of the control cells (Fig. 3 C). Namely, the tomosyn complex was more predominantly formed in the cells overexpressing HA-tomosyn than in the control cells, and conversely the SNARE complex was less predominantly formed in the cells overexpressing HA-tomosyn than in the control cells. Moreover, overexpression of myc-ROCK-Δ3 increased the formation of the tomosyn complex and conversely reduced the formation of the SNARE complex (Fig. 3 C). These results indicate that ROCK inhibits the formation of the SNARE complex through enhancing the formation of the tomosyn complex, and thereby blocks the fusion of the plasmalemmal precursor vesicles with the plasma membrane of growth cones.

To clarify the molecular link between the tomosyn complex and ROCK, we attempted to identify the substrate for ROCK. We assumed that syntaxin-1 is phosphorylated by ROCK to form the stable tomosyn complex. Consistently, recombinant syntaxin-1 was phosphorylated by ROCK time dependently (Fig. 4 A, a). 1 mol of phosphate was maximally incorporated into 1 mol of syntaxin-1. To map the potential phosphorylation sites, we used site-directed mutagenesis to generate seven syntaxin-1 mutants, in which serine or threonine was replaced to alanine, according to the consensus recognition sequence for ROCK. The phosphorylation of the S14A mutant by ROCK was markedly reduced in comparison with that of the other mutants, indicating that S14 is at least one of the in vitro phosphorylation sites of syntaxin-1 (unpublished data). Then, we examined the effect of the ROCK-induced phosphorylation of syntaxin-1 on its binding to tomosyn. The phosphorylated form bound to tomosyn about fivefold more than the nonphosphorylated form (Fig. 4 A, b). The apparent Kd values of the phosphorylated and nonphosphorylated forms were ~10 and 120 nM, respectively. In contrast, both the phosphorylated and nonphosphorylated forms bound to VAMP-2 to

knock-down. The fluorescence intensity of tomosyn of the NG108 cells expressing GFP were compared with that of the untransfected cells in the same field of view. (Bc) Quantitative analysis of the neurite length of NG108 cells as in Ac. *, $P < 0.01$. (Bd) Quantitative analysis of the number of neurites per cell of NG108 cells as in Ad.

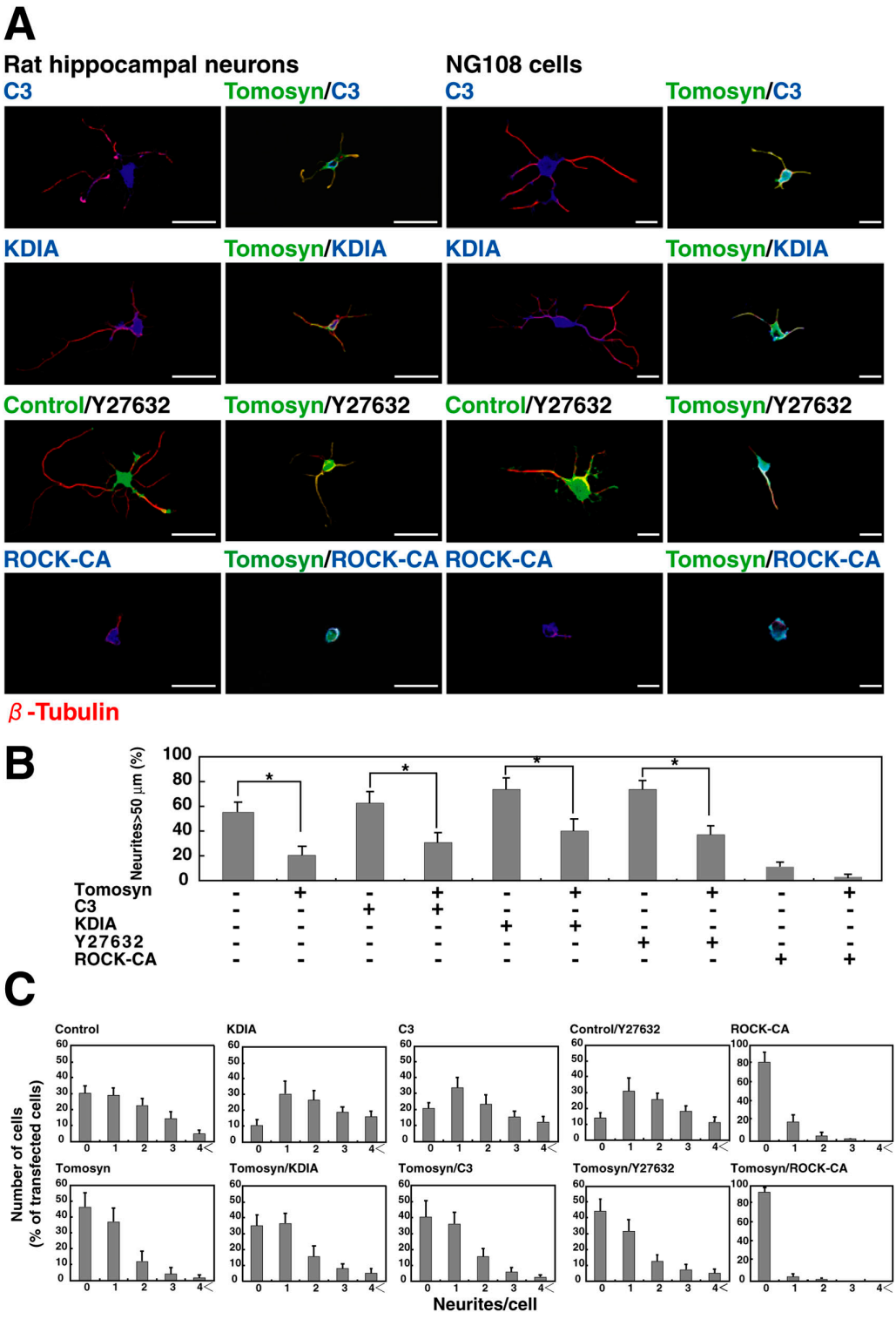

Figure 2. **Involvement of ROCK in the inhibitory effect of tomosyn on neurite outgrowth.** (A) Functional interaction between tomosyn and ROCK. Primary cultured rat hippocampal neurons were transfected with myc-C3, myc-ROCK-KDIA, or myc-ROCK-Δ3 (ROCK-CA) alone, or were cotransfected with HA-tomosyn, and were cultured for 24 h. NG108 cells were transfected with myc-C3, myc-ROCK-KDIA, or myc-ROCK-Δ3 (ROCK-CA) alone, or cotransfected with HA-tomosyn, cultured in DME containing 1 mM db-cAMP for 48 h, and allowed to extend neurites. Primary cultured rat hippocampal neurons and NG108 cells were transfected with HA-tomosyn or a null HA plasmid (Control) and were cultured in DME containing 20 μM Y27632 for 24 h. The cotransfected cells were identified by immunostaining of HA (green) and myc (blue), and their MT structures (red) were examined by immunostaining of β-tubulin (red). Bars, 20 μm. (B) Quantitative analysis of the neurite length of NG108 cells as in Fig. 1, Ac. *, $P < 0.01$. (C) Quantitative analysis of the number of neurites per cell of NG108 cells as in Fig. 1, Ad.

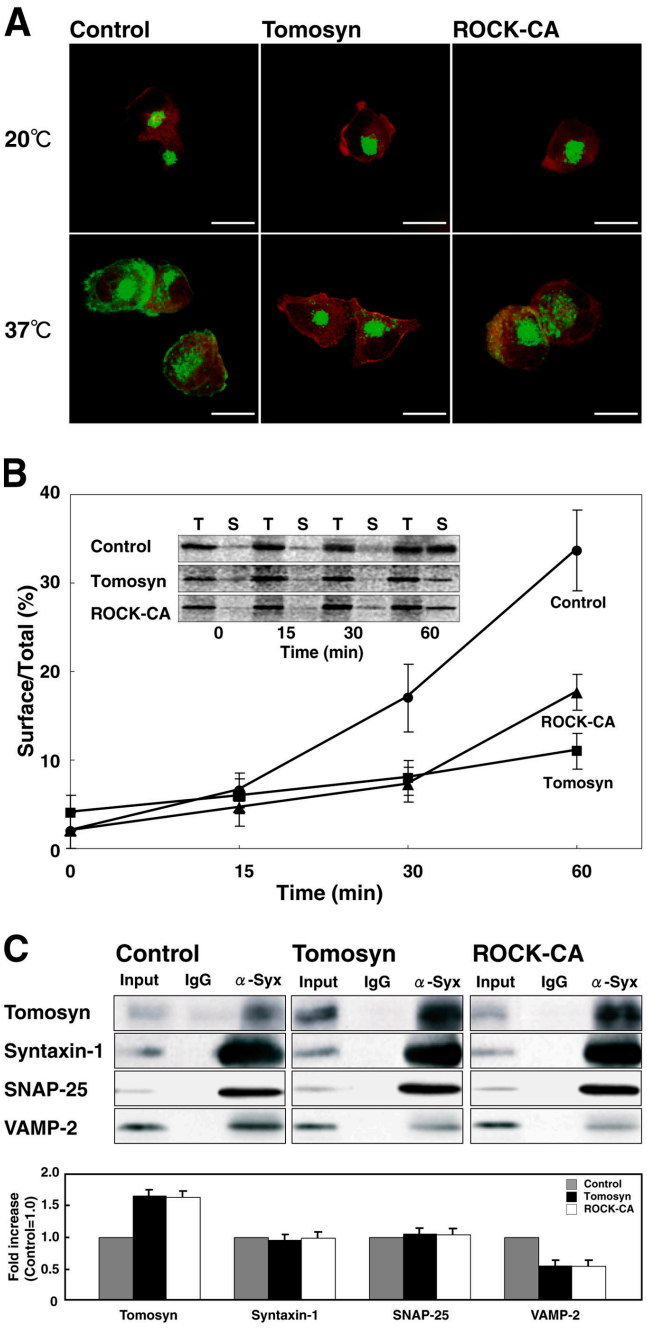

Figure 3. **Inhibition of vesicle transport by tomosyn and ROCK.** (A) Transport of VSV-G in NG108 cells. NG108 cells were cotransfected with GFP-VSV-G and either HA-tomosyn, myc-ROCK-Δ3 (ROCK-CA), or a null HA plasmid (Control). At 4 h after the transfection, the cells were incubated at 20°C for 2 h. Parallel samples were transferred to 37°C immediately after the 20°C incubation. The cotransfected cells were identified by the expression of GFP (green) and either immunostaining of HA or myc (red), and the distributions of GFP-VSV-G were examined. Bars, 20 μm. (B) Kinetics of VSV-G cell surface transport in NG108 cells. NG108 cells were cotransfected with VSV-G and either HA-tomosyn, myc-ROCK-Δ3 (ROCK-CA), or a null HA plasmid (Control). At 4 h after the transfection, the cells were labeled with [^{35}S]methionine and were incubated for indicated periods of time. To detect cell surface VSV-G, the cell surface was biotinylated. After the biotinylation, the cells were lysed and total VSV-G was collected by immunoprecipitation with the anti-VSV-G mAb. Cell surface–biotinylated VSV-G was recovered with streptavidin-agarose beads from total VSV-G. Biotinylated (S: surface) and total (T: 20% of total) VSV-G were separated by SDS-PAGE and the intensity of each band was quantified. (C) Quantification of the formation of SNARE and tomosyn complexes in NG108 cells. NG108 cells were transfected with HA-tomosyn, myc-ROCK-Δ3 (ROCK-CA), or a null HA plasmid (Control), cultured in DME containing 1 mM db-cAMP for 48 h, and allowed to extend neurites. Cells were lysed and immunoprecipitated with the anti-syntaxin-1 mAb or the control mouse IgG, followed by immunoblotting with the indicated antibodies. The quantification of immunoblot is shown on the bottom.

similar extents (Fig. 4 A, c). These results indicate that syntaxin-1 is phosphorylated by ROCK and forms a stable tomosyn complex, at least in a cell-free system.

Lysophosphatidic acid (LPA) activates the Rho–ROCK pathway and thereby induces collapse of growth cones and retraction of neurites (Hirose et al., 1998; Zhang et al., 2003). Therefore, we examined whether the phosphorylation of syntaxin-1 by ROCK is induced by LPA in intact cells. When NG108 cells expressing exogenous syntaxin-1 were stimulated by LPA, the phosphorylation of syntaxin-1 was significantly enhanced (Fig. 4 B, a). The phosphorylation of the S14A mutant was not affected in response to LPA, indicating that S14 is at least one of the major phosphorylation sites of syntaxin-1 in intact cells. This LPA-induced phosphorylation of syntaxin-1 at S14 was inhibited by Y27632, a specific ROCK inhibitor (Fig. 4 B, b). In addition, overexpression of HA-S14A–syntaxin-1 potently antagonized the inhibitory effect of tomosyn on the neurite outgrowth in NG108 cells (Fig. 4 C, a–c). Furthermore, the tomosyn complex was more predominantly formed in the cells stimulated by LPA than in the control cells, and conversely the SNARE complex was less predominantly formed in the cells stimulated by LPA than in the control cells (Fig. 4 D). These results indicate that syntaxin-1 is indeed phosphorylated by ROCK and forms the stable tomosyn complex in response to LPA in intact cells.

Then, we questioned where the stable tomosyn complex is formed in extension of neurites, and analyzed the subcellular localization of tomosyn in extending neurites, in comparison with those of the phosphorylated and nonphosphorylated forms of syntaxin-1, VAMP-2, actin filaments (F-actin), microtubules (MTs), and Sec6/8. Sec6/8 are the components of exocyst essential for polarized vesicle targeting (Hsu et al., 1999). A single neurite was visualized at a high magnification (Fig. 5 A). The Sec6/8 exocyst complex was highly concentrated at the leading edges of growth cones where active vesicle exocytosis occurs. Tomosyn localized just behind the Sec6/8 exocyst complex at the palm of growth cones. Syntaxin-1 phosphorylated at S14 specifically localized at the palm of the growth cones. The nonphosphorylated form of syntaxin-1 diffusely localized along the plasma membrane of neurites as described previously (Garcia et al., 1995). VAMP-2 was scattered throughout the cytoplasm and in the neurites. MTs extended to the area where tomosyn localized. F-actin localized from the palm to the leading edges of the growth cones. Thus, tomosyn colocalizes with the phosphorylated form of syntaxin-1 and F-actin at the palm of the growth cones. Taking an example of chemotaxing neutrophils, activated ROCK localizes at the cell posterior during directional cell movement (Xu et al., 2003). This is coupled

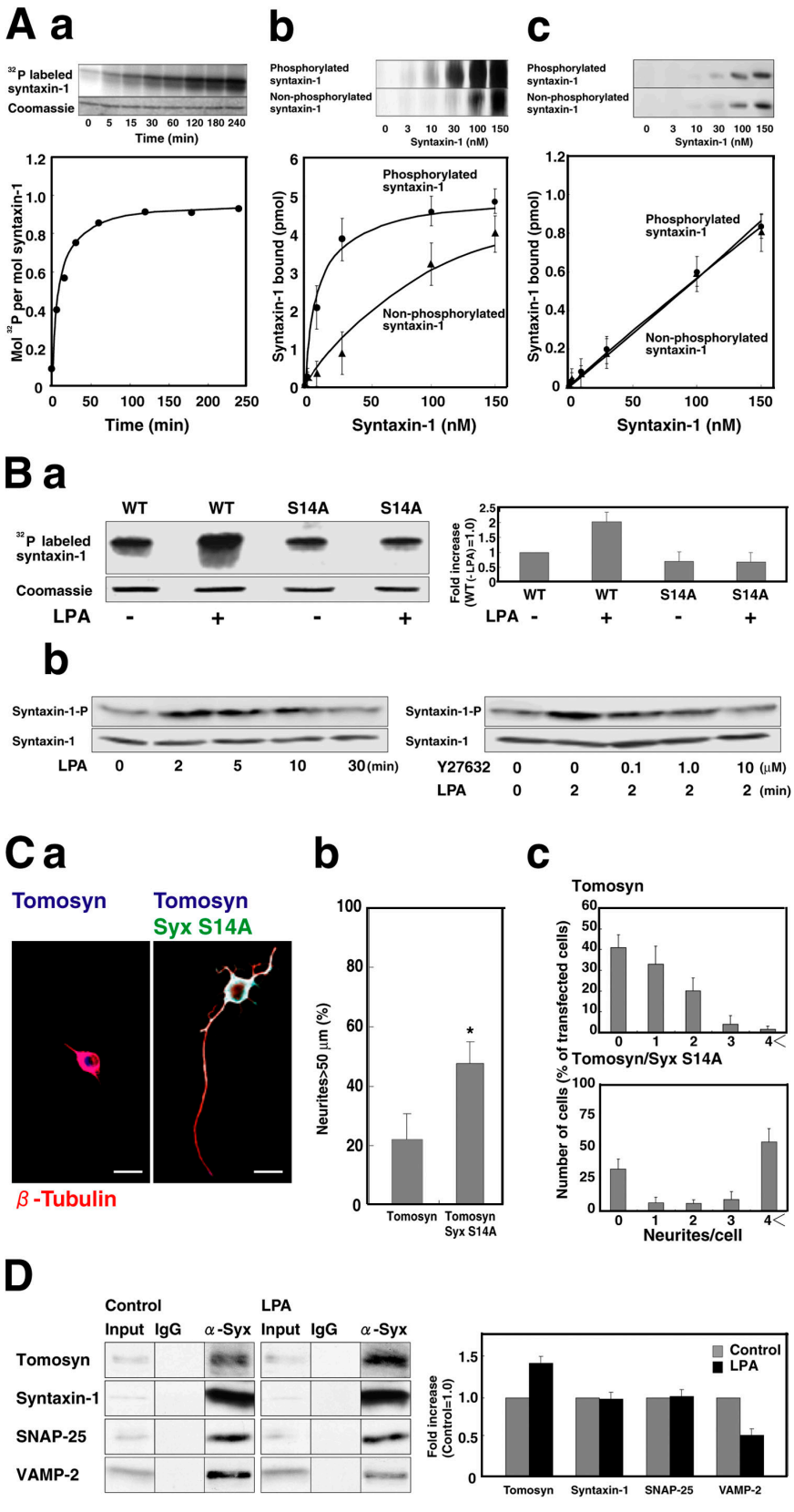

Figure 4. **Molecular link between the tomosyn complex and ROCK in the LPA-induced retraction of neurites.** (A) Phosphorylation of syntaxin-1 by ROCK in a cell-free system and increase of the affinity of syntaxin-1 for tomosyn. (Aa) Syntaxin-1 was phosphorylated by ROCK for indicated periods of time. After the reaction, the reaction mixture was subjected to SDS-PAGE followed by protein staining and autoradiography (top). Gel slices containing labeled syntaxin-1 were scintillation counted, and the molar amount of ^{32}P incorporated into syntaxin-1 was calculated and plotted (bottom). (Ab) Various quantities of the nonphosphorylated or phosphorylated form of syntaxin-1 were incubated with tomosyn (5 pmol) on a nitrocellulose membrane sheet. The syntaxin-1 bound to tomosyn was detected by immunoblotting with the anti-syntaxin-1 mAb (top). The quantification of immunoblot is shown on the bottom. (Ac) Various quantities of the nonphosphorylated or phosphorylated form of syntaxin-1 were incubated with VAMP-2 (5 pmol) on a nitrocellulose membrane sheet. The syntaxin-1 bound to VAMP-2 was detected by immunoblotting with the anti-syntaxin-1 mAb (top). The quantification of immunoblot is shown on the bottom. (B) Phosphorylation of syntaxin-1 in response to LPA in intact cells. (Ba) NG108 cells were transfected with HA-syntaxin-1 or HA-S14A-syntaxin-1, cultured in DME containing 1 mM db-cAMP for 48 h, and allowed to extend neurites. The cells were labeled with ^{32}P and were stimulated by 5 μM LPA for 5 min. The cells were lysed and immunoprecipitated with the anti-HA mAb. The immunoprecipitated samples were subjected to SDS-PAGE followed by protein staining and autoradiography. The relative intensity of autoradiography is shown on the right. (Bb) NG108 cells were cultured in DME containing 1 mM db-cAMP for 48 h and were allowed to extend neurites. On the left, the cells were stimulated by 5 μM LPA for indicated periods of time. Cells were collected in the SDS-PAGE sample buffer and subjected to immunoblotting with the anti-S14-phosphospecific pAb (top) and the anti-syntaxin-1 mAb (bottom). On the right, the cells were treated with indicated concentrations of Y27632 for 30 min and stimulated by 5 μM LPA for 2 min. Cells were lysed and analyzed as described above. (C) Prevention of the inhibitory effect of tomosyn on neurite outgrowth by S14A-syntaxin-1. (Ca) NG108 cells were transfected with myc-tomosyn alone or were cotransfected with HA-S14A-syntaxin-1 (Syx S14A), cultured in DME containing 1 mM db-cAMP for 48 h, and allowed to extend neurites. The cotransfected cells were identified by immunostaining of HA (green) and immunostaining of myc (blue), and their MT structures (red) were examined by immunostaining of β-tubulin (red). Bars, 20 μm. (Cb) Quantitative analysis of the neurite length of NG108 cells as in Fig. 1, Ac. *, $P < 0.01$. (Cc) Quantitative analysis of the number of neurites per cell of NG108 cells as in Fig. 1, Ad. (D) Enhancement of the formation of the tomosyn complex in response to LPA in intact cells. NG108 cells were cultured in DME containing 1 mM db-cAMP for 48 h and were allowed to extend neurites. Cells were stimulated by 5 μM LPA for 5 min. Cells were lysed and immunoprecipitated with the anti-syntaxin-1 mAb or the control mouse IgG, followed by immunoblotting with the indicated antibodies. The quantification of immunoblot is shown on the right.

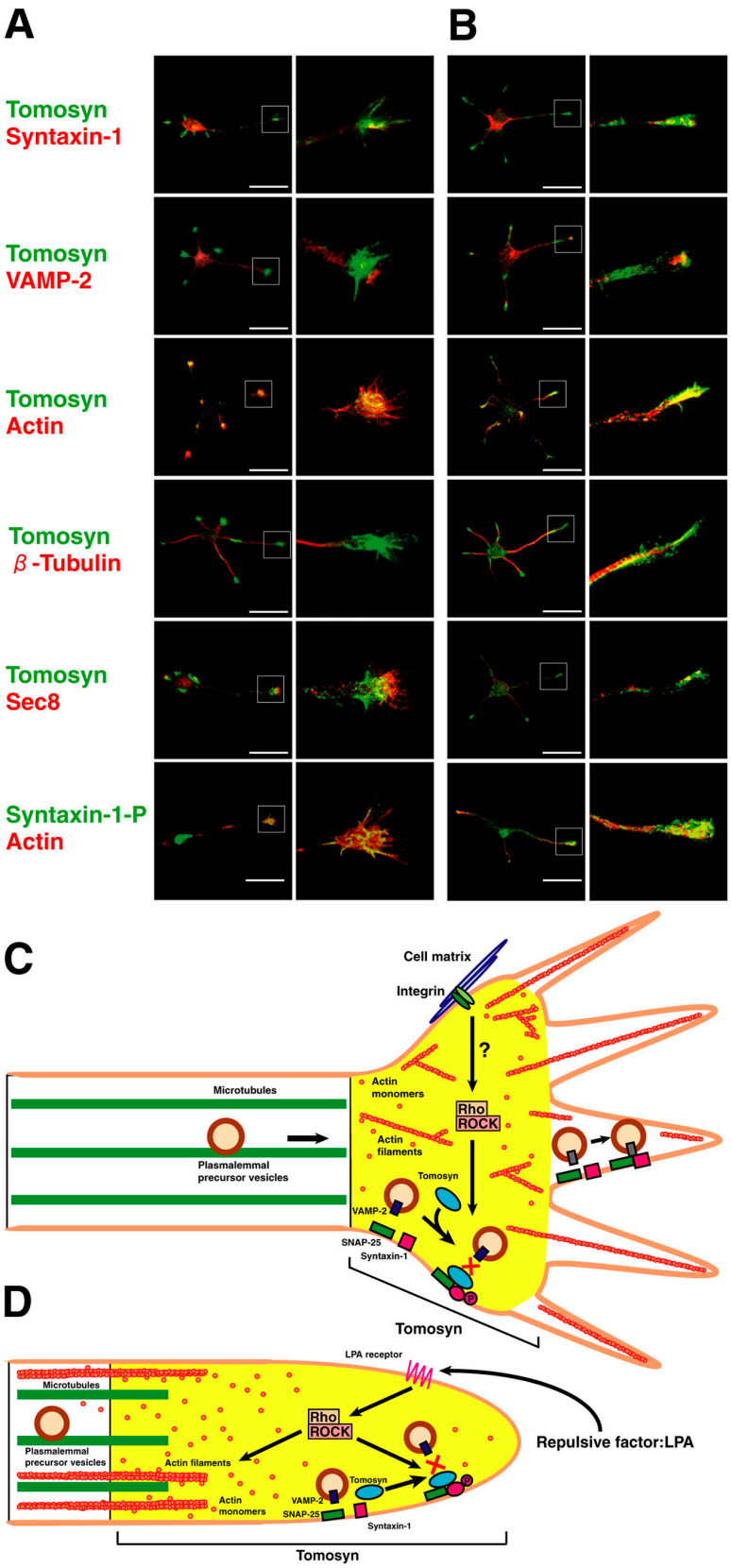

Figure 5. **Localization of tomosyn in extending and retracting neurites and models of a role of tomosyn in extension and retraction of neurites.** (A) Localization of tomosyn in extending neurites. Rat hippocampal neurons cultured for 36 h were costained with tomosyn (green) and the indicated antibodies (red). Bars, 20 μm. (B) Localization of tomosyn in retracting neurites. Neurons cultured for 36 h were stimulated by 1 μM LPA for 5 min and were subsequently costained with tomosyn (green) and the indicated antibodies (red). Bars, 20 μm. (C) A model of a role of tomosyn in extension of neurites. During extension of neurites, tomosyn localizes at the palm of growth cones and forms the stable tomosyn complex, thus inhibiting the formation of the SNARE complex and the subsequent fusion of plasmalemmal precursor vesicles with the plasma membrane there. As a result, plasmalemmal precursor vesicles fuse with the plasma membrane of the leading edges of growth cones. (D) A model of a role of tomosyn in LPA-induced retraction of neurites. During retraction of neurites, LPA activates the Rho–ROCK system, which induces the actomyosin-based contractility to enhance growth cone collapse and neurite retraction. On the other hand, the activated Rho–ROCK system phosphorylates syntaxin-1 on the plasma membrane of the retracted neurites, forming the stable tomosyn complex spreading along the plasma membrane of retracted neurites. The formation of the stable tomosyn complex then inhibits the formation of the SNARE complex and the subsequent fusion of plasmalemmal precursor vesicles with the plasma membrane of retracted neurites. As a result, the inhibition of fusion of plasmalemmal precursor vesicles and the actomyosin-based contractility enhance the retraction of neurites cooperatively.

to an actomyosin-based contractility at the cell posterior, which reduces the adhesion of the cell posterior to the substratum, allowing the cells to be released and to retract in the direction of movement. By analogy, ROCK might be similarly activated in the growth cone's posterior, the palm of growth cones. Together, it is likely that ROCK is locally activated at the palm of growth cones and phosphorylates syntaxin-1 to form the stable tomosyn complex there.

The last question is whether activated ROCK affects the localization of the stable tomosyn complex. ROCK is activated in response to extracellular signals, such as LPA, through their receptors, and to substratum, such as collagen, through integrins in fibroblasts and epithelial cells (Etienne-Manneville and Hall, 2002). Also in neurons, ROCK is activated in response to LPA, causing collapse of growth cones and retraction of neurites (Hirose et al., 1998; Zhang et al., 2003). Lastly, we examined whether the localization of tomosyn and the phosphorylated form of syntaxin-1 are affected in response to LPA in hippocampal neurons. LPA caused collapse of growth cones and retraction of neurites (Fig. 5 B). The localization of tomosyn and the phosphorylated form of syntaxin-1 spread along the plasma membrane of retracted neurites. In contrast, the localization of the nonphosphorylated form of syntaxin-1, VAMP-2, or Sec6/8 did not show such a drastic change after the stimulation by LPA. These results suggest that the site for the formation of the stable tomosyn complex in retraction of neurites is determined by the activation of ROCK through LPA receptors.

The present results indicate that tomosyn forms the stable complex with syntaxin-1 phosphorylated by ROCK and reduces the availability of syntaxin-1 for the formation of the SNARE complex, resulting in the inhibition of the fusion of plasmalemmal precursor vesicles with the plasma membrane where the stable tomosyn complex forms. In extension of neurites, vesicles including the plasmalemmal precursor vesicles are transported along MTs by MT-associated motors to the plasma membrane of growth cones (Horton and Ehlers, 2003; Fig. 5 C). Once vesicles are delivered to the ends of the MTs at the palm of growth cones, they might be released from the MTs. However, fusion of these released vesicles with the plasma membrane at the palm of growth cones is blocked by tomosyn, which forms the stable complex with syntaxin-1 phosphorylated by ROCK. The vesicles are transferred from MTs to the actin cytoskeleton and are distributed to the plasma membrane of the leading edges of growth cones, resulting in extension of neurites. In contrast, in retraction of neurites, ROCK is activated in response to extracellular signals, such as LPA, through their receptors and induces the actomyosin-based contractility to enhance collapse of growth cones and retraction of neurites (Fig. 5 D). On the other hand, activated ROCK phosphorylates syntaxin-1 on the plasma membrane of retracted neurites, forming the stable tomosyn complex that spreads along the plasma membrane of the retracted neurites. The formation of the stable tomosyn complex then inhibits the formation of the SNARE complex and the subsequent fusion of plasmalemmal precursor vesicles with the plasma membrane of the retracted neurites. As a result, the inhibition of fusion of plasmalemmal precursor vesicles and the actomyosin-based contractility enhance the retraction of neurites cooperatively. If this inhibition of the vesicle fusion does not accompany the actomyosin-based contractility, the oversupplied membrane addition makes neurites flabby. Of course, there might additionally be a mechanism that enhances endocytosis of extra membranes in retraction of neurites.

Materials and methods

Construction of expression vectors

To generate mammalian expression vectors for tomosyn (pCMV-HA-tomosyn and pcDNA3-HA-tomosyn), the full-length of m-tomosyn cDNA was subcloned into the pCMV-HA or pcDNA3-HA vector, respectively. The cDNAs for syntaxin-1A mutants, in which Thr at 5, 21, and 118 aa residues and Ser at 14, 59, and 91 aa residues were replaced to Ala, were generated using a sitedirected mutagenesis kit (Stratagene) and subcloned into pGEX-2T and pCMVHA vectors. The pEF-BOS-myc-C3 was constructed (Komuro et al., 1996). The pCAG-myc-ROCK-Δ3 and pCAG-myc-ROCK-KDIA were provided by Dr. S. Narumiya (Kyoto University Faculty of Medicine, Kyoto, Japan).

Knock-down of tomosyn by the RNA interference method

The mammalian expression vector pSIREN-RetroQ (CLONTECH Laboratories, Inc.), which contains a GFP gene for the selection of transfected cells, was used for expression of small interfering RNA (siRNA) in NG108 cells. Inserts were used as follows: m-tomosyn gene-specific insert was a 21-nt sequence corresponding to nt 2478–2498 (5′-GCGGTACTATATTGAGGTTAA-3′) of m-tomosyn cDNA, which was separated by a 10-nt noncomplementary spacer (5′-TTGATATCCG-3′) from the reverse complement of the same 21-nt sequence. A control (Scramble) insert was a 21-nt sequence (5′-GACGTTATCGGTATGATATAG-3′) with no significant homology to any mammalian gene sequence, which was separated by a 10-nt noncomplementary spacer (5′-TTGATATCCG-3′) from the reverse complement of the same 21-nt sequence.

Quantification of neurites

After the 2-d db-cAMP treatment, NG108 cells were processed (Martinez-Arca et al., 2000). Images were captured using a confocal laser scanning microscope (Radiance 2000; Bio-Rad Laboratories) using a 60× oil immersion objective lens. Collected data were exported as 8-bit TIFF files and were processed using Adobe Photoshop® software. The assay for neurite outgrowth was performed on 100 cells randomly chosen in each group. The number of primary neurites per cell was defined as the number of thin cell processes with a length >20 μm. The length of individual neurites for each cell was measured by use of the NIH Image software. Neurite length was defined as the traced distance from the neurite tip to the point where neurite emanated from the cell body. The statistical significance of differences between each group was analyzed by the two-tailed *t* test.

Assay for VSV-G transport

NG108 cells were transfected with pAR vector encoding either GFP-VSV-G or VSV-G and assayed (Hirschberg et al., 1998). Where indicated, the cells were pulse labeled with [35S]methionine (0.1 mCi/ml) (Tran35S label; ICN Biomedicals) at 37°C for 10 min, chased at 20°C or 37°C for indicated periods of time, and analyzed. To detect surface VSV-G, biotinylation was performed by incubating the cells with 0.5 mg/ml Sulfo-NHS-Biotin (Pierce Chemical Co.) in PBS at 4°C for 30 min and quenched with 50 mM NH4Cl in PBS. The cells were lysed with a RIPA buffer. Total VSV-G was immunoprecipitated with a mouse anti-VSV-G mAb (P5D4), washed, eluted with 0.1 ml of 1% SDS in TBS at 90°C for 3 min, and diluted with 1 ml of 1% Triton X-100 in TBS. Biotinylated VSV-G was recovered with streptavidin-agarose beads (Sigma-Aldrich) and surface VSV-G was eluted with the SDS sample buffer.

Assay for the formation of SNARE and tomosyn complexes

The lysate of NG108 cells was prepared using a lysis buffer (20 mM Hepes, pH 7.4, 90 mM KOAc, 2 mM $Mg(OAc)_2$, 0.5 mM EGTA, 50 mM NaF, 2 mM Na_3VO_4, and 1% CHAPS; Fujita et al., 1998). The lysates were incubated with an anti-syntaxin-1 mAb (Synaptic Systems) at 4°C for 2 h. The immune complexes were precipitated with protein G–Sepharose beads (Amersham Biosciences) at 4°C for 1 h, washed with the lysis buffer, resolved in 5–20% gradient SDS-PAGE, and analyzed by immunoblotting with an anti-tomosyn pAb (Fujita et al., 1998), an anti-VAMP-2 pAb (Synaptic systems), an anti-SNAP-25 pAb (Calbiochem), and an anti-syntaxin-1 pAb (Calbiochem).

Assay for the binding of syntaxin-1 to tomosyn and VAMP-2

Overlay assay was performed (Fujita et al., 1998). The Sf9 cells expressing tomosyn were collected and boiled with the SDS sample buffer, followed by centrifugation. The GST-VAMP-2 protein was generated in *Escherichia coli* (Fujita et al., 1998). Tomosyn or VAMP-2 (5 pmol each) was subjected to SDS-PAGE and blotted onto a nitrocellulose membrane sheet. The sheet

was incubated with various quantities of syntaxin-1 in 1 ml of TBS containing 5% skim milk for 2 h. The amount of syntaxin-1 bound to the sheet was detected by immunoblotting with the anti-syntaxin-1 mAb. The intensity of the bands was measured with CS-9000 (Shimazu).

Phosphorylation of syntaxin-1 by ROCK in a cell-free system

Syntaxin-1 was phosphorylated by ROCK in a cell-free system (Sumi et al., 2001). HEK293 cells were transiently transfected with pCAG-myc-ROCK-Δ3 plasmid. Cells were lysed in the lysis buffer and immunoprecipitated with an anti-myc mAb. Myc-ROCK-Δ3 (5 pmol)–bound protein G–Sepharose beads (50 μl slurry) were washed with a kinase buffer (50 mM Tris/HCl, pH 7.5, 7 mM $MgCl_2$, 1 mM DTT, 0.06% CHAPS, and 1 mM EDTA) and were incubated at 30°C for indicated periods of time in 100 μl of the kinase buffer containing 50 μM γ[^{32}P]ATP (0.5–1.2 × 10^3 cpm/pmol; Amersham Biosciences) and 30 pmol syntaxin-1 as a substrate. The reaction was stopped by the addition of the SDS sample buffer and boiled for 5 min. Each sample was subjected to SDS-PAGE, followed by protein staining with Coomassie brilliant blue and autoradiography. Relevant gel slices were excised and scintillation counted to determine the radioactivity incorporated into syntaxin-1.

Phosphorylation of syntaxin-1 in intact cells

NG108 cells were transfected with either pCMV-HA-syntaxin-1A or pCMV-HA-S14A-syntaxin-1A, cultured in DME containing 1 mM db-cAMP for 48 h, and allowed to extend neurites. The cells were washed three times with phosphate-free DME and were incubated for 30 min in the phosphate-free DME containing 1 mM db-cAMP and 1× HT. Thereafter, [^{32}P]orthophosphate (phosphorus-32; Amersham Biosciences) was added at a concentration of 0.5 mCi/ml in the phosphate-free DME containing 1 mM db-cAMP and 1× HT. Cells were cultured for 4 h and stimulated by 5 μM LPA for 5 min. Cells were lysed with RIPA buffer and immunoprecipitated with the anti-HA mAb. The immunoprecipitates were subjected to SDS-PAGE, followed by autoradiography.

Assay for the phosphorylation of syntaxin-1 at serine 14 in vivo

NG108 cells were cultured in DME containing 1 mM db-cAMP for 48 h and were allowed to extend neurites. The cells were preincubated with or without various concentrations of Y27632 for 30 min and were then stimulated by 5 μM LPA for indicated periods of time. Cells were lysed with the SDS-PAGE sample buffer and were subjected to immunoblotting with the anti-phosphorylated syntaxin-1 (S14-phosphospecific) pAb (Foletti et al., 2000).

We thank Dr. R.H. Scheller (Genentech, San Francisco, CA) for providing us with an anti-phosphorylated syntaxin-1 pAb.

This work was supported by grants-in-aid for Scientific Research and for Cancer Research from the Ministry of Education, Culture, Sports, Science, and Technology, Japan (2003). T. Sakisaka is a recipient of a Human Frontier Science Program Career Development Award (2003).

Submitted: 3 May 2004
Accepted: 25 May 2004

References

Bito, H., T. Furuyashiki, H. Ishihara, Y. Shibasaki, K. Ohashi, K. Mizuno, M. Maekawa, T. Ishizaki, and S. Narumiya. 2000. A critical role for a Rho-associated kinase, p160ROCK, in determining axon outgrowth in mammalian CNS neurons. *Neuron.* 26:431–441.

Chen, Y.A., and R.H. Scheller. 2001. SNARE-mediated membrane fusion. *Nat. Rev. Mol. Cell Biol.* 2:98–106.

Da Silva, J.S., M. Medina, C. Zuliani, A. Di Nardo, W. Witke, and C.G. Dotti. 2003. RhoA/ROCK regulation of neuritogenesis via profilin IIa–mediated control of actin stability. *J. Cell Biol.* 162:1267–1279.

Etienne-Manneville, S., and A. Hall. 2002. Rho GTPases in cell biology. *Nature.* 420:629–635.

Foletti, D.L., R. Lin, M.A. Finley, and R.H. Scheller. 2000. Phosphorylated syntaxin 1 is localized to discrete domains along a subset of axons. *J. Neurosci.* 20:4535–4544.

Fujita, Y., H. Shirataki, T. Sakisaka, T. Asakura, T. Ohya, H. Kotani, S. Yokoyama, H. Nishioka, Y. Matsuura, A. Mizoguchi, et al. 1998. Tomosyn: a syntaxin-1-binding protein that forms a novel complex in the neurotransmitter release process. *Neuron.* 20:905–915.

Futerman, A.H., and G.A. Banker. 1996. The economics of neurite outgrowth—the addition of new membrane to growing axons. *Trends Neurosci.* 19:144–149.

Garcia, E.P., P.S. Mcpherson, T.J. Chilcote, K. Takei, and P. De Camilli. 1995. rbSec1A and B colocalize with syntaxin 1 and SNAP-25 throughout the axon, but are not in a stable complex with syntaxin. *J. Cell Biol.* 129:105–120.

Goslin, K., and G. Banker. 1989. Experimental observations on the development of polarity by hippocampal neurons in culture. *J. Cell Biol.* 108:1507–1516.

Hirose, M., T. Ishizaki, N. Watanabe, M. Uehata, O. Kranenburg, W.H. Moolenaar, F. Matsumura, M. Maekawa, H. Bito, and S. Narumiya. 1998. Molecular dissection of the Rho-associated protein kinase (p160ROCK)-regulated neurite remodeling in neuroblastoma N1E-115 cells. *J. Cell Biol.* 141:1625–1636.

Hirschberg, K., C.M. Miller, J. Ellenberg, J.F. Presley, E.D. Siggia, R.D. Phair, and J. Lippincott-Schwartz. 1998. Kinetic analysis of secretory protein traffic and characterization of Golgi to plasma membrane transport intermediates in living cells. *J. Cell Biol.* 143:1485–1503.

Horton, A.C., and M.D. Ehlers. 2003. Neuronal polarity and trafficking. *Neuron.* 40:277–295.

Hsu, S.C., C.D. Hazuka, D.L. Foletti, and R.H. Scheller. 1999. Targeting vesicles to specific sites on the plasma membrane: the role of the sec6/8 complex. *Trends Cell Biol.* 9:150–153.

Komuro, R., T. Sasaki, K. Takaishi, S. Orita, and Y. Takai. 1996. Involvement of Rho and Rac Small G proteins and Rho GDI in Ca^{2+}-dependent exocytosis from PC12 cells. *Genes Cells.* 1:943–951.

Martinez-Arca, S., P. Alberts, A. Zahraoui, D. Louvard, and T. Galli. 2000. Role of tetanus neurotoxin insensitive vesicle-associated membrane protein (TI-VAMP) in vesicular transport mediating neurite outgrowth. *J. Cell Biol.* 149: 889–900.

Masuda, E.S., B.C. Huang, J.M. Fisher, Y. Luo, and R.H. Scheller. 1998. Tomosyn binds t-SNARE proteins via a VAMP-like coiled coil. *Neuron.* 21:479–480.

Nirenberg, M., S. Wilson, H. Higashida, A. Rotter, K. Krueger, N. Busis, R. Ray, J.G. Kenimer, and M. Adler. 1983. Modulation of synapse formation by cyclic adenosine monophosphate. *Science.* 222:794–799.

Sumi, T., K. Matsumoto, and T. Nakamura. 2001. Specific activation of LIM kinase 2 via phosphorylation of threonine 505 by ROCK, a Rho-dependent protein kinase. *J. Biol. Chem.* 276:670–676.

Xu, J., F. Wang, A. Van Keymeulen, P. Herzmark, A. Straight, K. Kelly, Y. Takuwa, N. Sugimoto, T. Mitchison, and H.R. Bourne. 2003. Divergent signals and cytoskeletal assemblies regulate self-organizing polarity in neutrophils. *Cell.* 114:201–214.

Zhang, X.F., A.W. Schaefer, D.T. Burnette, V.T. Schoonderwoert, and P. Forscher. 2003. Rho-dependent contractile responses in the neuronal growth cone are independent of classical peripheral retrograde actin flow. *Neuron.* 40:931–944.